ACS APPLIED MATERIALS & INTERFACES

Research Article

www.acsami.org

DNA Immobilization and Hybridization Detection by the Intrinsic Molecular Charge Using Capacitive Field-Effect Sensors Modified with a Charged Weak Polyelectrolyte Layer

Thomas S. Bronder,[†] Arshak Poghossian,[*,†,§] Sabrina Scheja,[†] Chunsheng Wu,[†,‡] Michael Keusgen,[∥] Dieter Mewes,[⊥] and Michael J. Schöning[†,§]

[†]Institute of Nano- and Biotechnologies, FH Aachen, Campus Jülich, 52428 Jülich, Germany

[‡]Biosensor National Special Laboratory, Key Laboratory for Biomedical Engineering of Ministry of Education, Department of Biomedical Engineering, Zhejiang University, Hangzhou 310027, China

[§]Peter Grünberg Institute (PGI-8), Research Centre Jülich GmbH, 52425 Jülich, Germany

[∥]Institute of Pharmaceutical Chemistry, Philipps University Marburg, 35032 Marburg, Germany

[⊥]Institute of Measurement and Automatic Control, Leibniz University Hannover, 30167 Hannover, Germany

Supporting Information

ABSTRACT: Miniaturized setup, compatibility with advanced micro- and nanotechnologies, and ability to detect biomolecules by their intrinsic molecular charge favor the semiconductor field-effect platform as one of the most attractive approaches for the development of label-free DNA chips. In this work, a capacitive field-effect EIS (electrolyte−insulator−semiconductor) sensor covered with a layer-by-layer prepared, positively charged weak polyelectrolyte layer of PAH (poly(allylamine hydrochloride)) was used for the label-free electrical detection of DNA (deoxyribonucleic acid) immobilization and hybridization. The negatively charged probe single-stranded DNA (ssDNA) molecules were electrostatically adsorbed onto the positively charged PAH layer, resulting in a preferentially flat orientation of the ssDNA molecules within the Debye length, thus yielding a reduced charge-screening effect and a higher sensor signal. Each sensor-surface modification step (PAH adsorption, probe ssDNA immobilization, hybridization with complementary target DNA (cDNA), reducing an unspecific adsorption by a blocking agent, incubation with noncomplementary DNA (ncDNA) solution) was monitored by means of capacitance−voltage and constant-capacitance measurements. In addition, the surface morphology of the PAH layer was studied by atomic force microscopy and contact-angle measurements. High hybridization signals of 34 and 43 mV were recorded in low-ionic strength solutions of 10 and 1 mM, respectively. In contrast, a small signal of 4 mV was recorded in the case of unspecific adsorption of fully mismatched ncDNA. The density of probe ssDNA and dsDNA molecules as well as the hybridization efficiency was estimated using the experimentally measured DNA immobilization and hybridization signals and a simplified double-layer capacitor model. The results of field-effect experiments were supported by fluorescence measurements, verifying the DNA-immobilization and hybridization event.

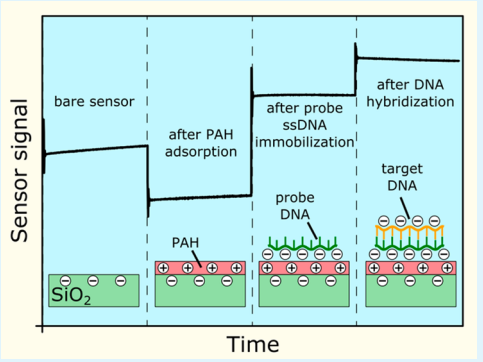

KEYWORDS: *DNA, hybridization, intrinsic molecular charge, label-free detection, field-effect capacitive sensor, polyelectrolyte, layer-by-layer technique*

1. INTRODUCTION

DNA (deoxyribonucleic acid) biosensors are considered as a very promising tool in many fields of applications ranging from diagnosis of genetic diseases, pathogen identification, and parental testing to drug screening and food industry.[1−4] The developed DNA-detection principles are very different: optical, electrochemical, impedimetric, spectrometric, and gravimetric methods are just a few of them.[5−11] The fundamental mechanism of many DNA-detection methods relies on the detection of the hybridization event in which a single-stranded probe DNA (ssDNA) binds specifically to a complementary single-stranded target DNA (cDNA), forming a double-stranded DNA (dsDNA) with a well-known helix structure. Generally, DNA-detection principles can be divided into labeled, where either probe- or target-DNA molecules are labeled with different markers, and label-free methods. Label-free methods have obvious advantages in terms of simplicity, rapidity and cost-efficiency.[12,13] One favorable possibility to detect unlabeled DNA molecules is the detection of their intrinsic molecular charge by means of semiconductor field-

Received: June 10, 2015
Accepted: August 26, 2015
Published: August 26, 2015

DOI: 10.1021/acsami.5b05146
ACS Appl. Mater. Interfaces 2015, 7, 20068−20075

effect devices (FED),[4,13] because DNA molecules are negatively charged in a wide pH range. FEDs based on an electrolyte−insulator−semiconductor (EIS) structure, like capacitive EIS sensors, ion-sensitive field-effect transistors, Si-nanowire transistors and light-addressable potentiometric sensors (LAPS), are charge-sensitive devices and have been widely applied for the detection of pH,[14,15] ion and analyte concentration in liquids[16−21] as well as charged molecules[4,22] or charged nanoparticles.[23,24] The ability of different kinds of FEDs for label-free detection of the DNA-hybridization event has been demonstrated in refs 25−35. In these devices, the adsorption or binding of DNA molecules on the gate surface of the FED changes the space-charge distribution in the semiconductor, resulting in a change of the output signal of the FED. However, due to the screening of the DNA charge by counterions in the solution, the DNA-hybridization signal strongly depends on the ionic strength of the solution and the distance between the charge of the DNA molecules and the gate surface.[4,30,36−38] In addition, because the DNA charge is distributed along the molecule length, the DNA-immobilization method and orientation of molecules will have a strong impact on the DNA-hybridization signal.[39−41] These problems can be overcome by the immobilization of ssDNA molecules preferentially flat to the FED surface as well as by readout of the hybridization signal in a low-ionic strength solution.

Direct electrostatic immobilization of DNA molecules onto the FED surface is, in general, impossible due to electrostatic repulsion forces between the DNA and the FED surface with typically negatively charged gate insulators (e.g., SiO_2, Ta_2O_5, Si_3N_4). Therefore, a modification of the sensor surface by means of layer-by-layer (LbL) electrostatic adsorption of a cationic polyelectrolyte/ssDNA bilayer and subsequent hybridization with cDNA molecules becomes more popular in FED-based DNA biosensors design.[25,32,42−45] In contrast to often applied covalent immobilization methods that require time-consuming, cost-intensive procedures and complicated chemistry for functionalization of the gate surface and/or probe ssDNA, the LbL electrostatic adsorption technique is easy, fast, and applicable for substrates with any shapes and form.[42,46,47] The suitability of FEDs for the detection of adsorptively immobilized DNA has been demonstrated by modifying the gate surface of an EIS sensor[25] and a floating-gate field-effect transistor[44] by the positively charged poly-L-lysine. However, the recorded DNA-immobilization and hybridization signals were small (several mVs). On the other hand, recently, a high sensor signal has been reported by electrostatic adsorption of ssDNA (83 mV)[32] and dsDNA (20 mV)[45] on a LAPS surface modified with the positively charged weak polyelectrolyte of PAH (poly(allylamine hydrochloride)). Although LAPS devices are capable for addressable and multispot measurements, some disadvantages, such as necessity of illumination of the semiconductor with a modulated light source, dependence of the LAPS signal on the modulation frequency and intensity of the light, cross-talk due to the possible internal reflections in the semiconductor, and complicated readout circuit, might limit their application fields.

In the present work, the simplest FED—the capacitive EIS sensor—modified with a LbL-prepared PAH layer is applied for a label-free detection of electrostatic adsorption of probe ssDNA molecules onto the gate surface and subsequent hybridization with cDNA molecules. The EIS sensor represents a (bio)chemically sensitive capacitor, which can be easily fabricated at low cost (usually, no photolithographic process steps or complicated encapsulation procedures are needed). Moreover, those sensors can be integrated with microfluidic cells on wafer level. In contrast to LAPS, a small AC (alternating current) voltage is applied to readout the EIS capacitance (no illumination with a modulated light is necessary). It can be expected that adsorptively immobilized probe ssDNA molecules will be preferentially flat-oriented on the EIS surface with negatively charged phosphate groups directed to the positively charged PAH molecules; the DNA nucleobases exposed to the surrounding solution allow to hybridize with their target cDNA molecules. As it has been discussed in refs 25, 32, 42−44, in the presence of a positively charged polyelectrolyte layer, both the Debye screening effect and the electrostatic repulsion between target and probe DNA molecules will be less effective, and therefore, a higher hybridization signal can be expected.

During experiments, each surface-modification step was monitored electrochemically in terms of signal direction and amplitude by using capacitance−voltage ($C-V$) and constant-capacitance (ConCap) measurements. In addition, the surface morphology of the PAH layer was studied by atomic force microscopy (AFM) and contact-angle measurements, while fluorescence measurements served as a reference method to verify the results of electrochemical detection of the DNA-immobilization and hybridization event.

2. EXPERIMENTAL SECTION

2.1. Chip Fabrication. EIS sensor chips consisting of an Al/p-Si/SiO_2 structure were fabricated from a p-Si wafer (boron doped) with crystallographic orientation ⟨100⟩ and a resistivity of 1−10 Ωcm. First, a SiO_2 gate oxide was thermally grown by dry oxidation process at 1000 °C for 30 min to form a 30 nm thick oxide layer. Then, the rear-side oxide layer was etched by HF and subsequently, a 300 nm Al layer was deposited to create an ohmic contact to the silicon substrate. The last step of the fabrication process was the separation of the wafer into single 10 × 10 mm chips. After fabrication, each chip was cleaned in ultrasonic bath with acetone, isopropyl alcohol, ethanol, and deionized (DI) water.

2.2. Measurement Setup and Electrochemical Characterization. For electrochemical characterization, the EIS chips were mounted into a homemade measurement cell and connected to the electrochemical workstation. The rear-side and nonactive area of the chip were isolated from the electrolyte solution by means of an O-ring. The effective contact area of the EIS chip with the solution was about 0.7 cm^2. Figure 1 shows a schematic cross section of the EIS structure and measurement setup including the electrochemical workstation (Zennium, Zahner Elektrik, Germany) and the reference electrode (liquid-junction Ag/AgCl electrode filled with 3 M KCl, Metrohm, Germany).

To reduce the influence of the charge-screening effect, the measurements were performed in low-ionic strength solution (1 mM

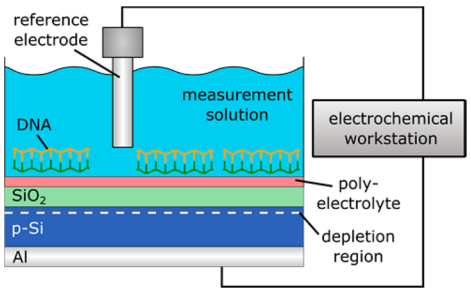

Figure 1. Cross-sectional illustration of the EIS sensor structure and measurement setup.

DOI: 10.1021/acsami.5b05146
ACS Appl. Mater. Interfaces 2015, 7, 20068−20075

and 10 mM NaCl, pH 5.45 adjusted by HCl, further referred as measurement solution). The pH value of all solutions was controlled with a MPC227 pH/Conductivity Meter (Mettler-Toledo, Germany). The surface-potential changes induced due to the surface-modification steps (PAH adsorption, probe ssDNA immobilization and target cDNA hybridization) were evaluated from the shifts of $C-V$ curves along the voltage axis in depletion region or directly recorded by means of ConCap mode measurements.

For the $C-V$ measurements, a DC (direct current) gate voltage ranging from −1.5 V to +0.5 V (steps of 100 mV) and a small superimposed AC voltage with an amplitude of 20 mV and a frequency of 60 Hz was applied between the reference electrode and the rear-side Al contact. The ConCap mode allows the real-time dynamic monitoring of the sensor signal, whereas the capacitance of the sensor is kept constant at a certain working point by varying the gate voltage using a feedback−control circuit. This working point (constant capacitance value) was chosen from the previously recorded $C-V$ curve, typically within the depletion region at approximately 60% of the maximum capacitance. The measurements were performed at room temperature in a dark Faraday box (to reduce the possible influence of ambient light and electromagnetic fields). All potential values are referred to the reference electrode.

2.3. LbL Adsorption of PAH/DNA Bilayer and Target cDNA Hybridization. The LbL technique provides a simple, fast, low-cost and efficient technique for the electrostatic assembling of polyions with alternating charge.[42,46,47] In this study, the LbL technique has been utilized for the adsorption of positively charged PAH macromolecules on the negatively charged SiO_2 gate insulator and the immobilization of negatively charged probe ssDNA molecules onto the positively charged PAH layer. The LbL-immobilized ssDNA molecules usually form flat elongated structures.[42] As a result, in low-ionic strength solutions used in this study, the full DNA charge could probably be positioned near the gate surface within the Debye length (approximately 3 and 10 nm in 10 and 1 mM solutions, respectively), yielding a higher sensor signal.

The schematic of the surface-modification steps is presented in Figure 2. Before polyelectrolyte adsorption, the surface of the SiO_2 layer was first activated with piranha solution (mixture of 60 μL H_2SO_4 (98%) and 30 μL H_2O_2 (35%)) by pipetting the freshly prepared mixture on the chip surface and incubating for at least 10 min at room temperature, followed by rinsing with DI water. This acid-treatment procedure was repeated three times. Then, 100 μL PAH solution (3 g/L PAH) was applied to the chip for 10 min to form the polyelectrolyte layer in accordance with the procedure described in ref 46. The PAH solution was prepared by dissolving of PAH (70 kDa, purchased from Sigma) in 100 mM NaCl, pH 5.45. At pH 5.45, the surface of SiO_2 can be considered to be enough negatively charged (the pH_{pzc} at point of zero charge of SiO_2 is between 2 and 3)[48] to provide electrostatic adsorption of almost fully charged PAH molecules.[49] The ionic strength of the PAH solution was chosen sufficiently high (100 mM NaCl) in order to achieve a higher amount of adsorbed polyelectrolyte molecules. After the PAH adsorption, the chip was washed again three times with measurement solution to remove nonattached molecules from the sensor surface, followed by an electrochemical characterization as described in section 2.2.

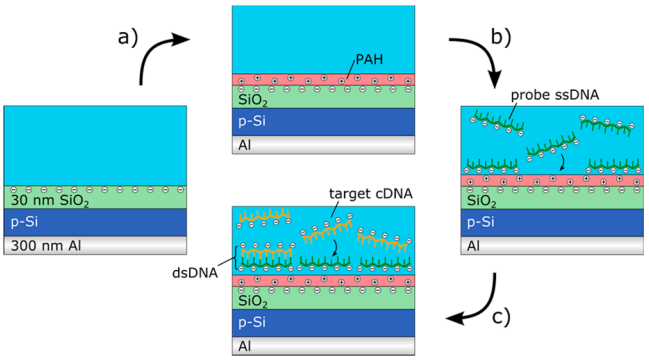

Figure 2. Schematic of the surface-modification steps: (a) PAH adsorption, (b) ssDNA immobilization, and (c) hybridization of complementary target cDNA with immobilized probe ssDNA molecules.

The density and homogeneity of the immobilized probe ssDNA layer will be mainly defined by the quality of the underlying PAH layer. Therefore, in separate experiments, the chip-surface morphology and roughness was characterized by AFM measurements before and after the PAH adsorption. Tapping-mode AFM images were taken using a BioMAT Workstation (JPK Instruments, Germany) and commercial NCH Pointprobe silicon cantilevers (Nanoworld, Switzerland). The surface roughness was quantified by using the root-mean-square value (rms) and the surface-area difference.

For immobilization of 20-mer probe ssDNA, 60 μL of 5 μM ssDNA solution was applied onto the PAH-modified chip surface. The DNA solution has been prepared by dilution of ssDNA molecules in 1 × TE buffer (mixture of 10 mM Tris (tris(hydroxymethyl)aminomethane) and 1 mM EDTA (ethylenediaminetetraacetic acid) in DI water, adjusted to pH 8). After 60 min of incubation, the chip was washed three times with measurement solution to remove unattached probe ssDNA molecules.

For hybridization, the chip surface covered with the PAH/ssDNA bilayer was incubated with fully matched target cDNA solution (5 μM 20-mer cDNA dissolved in 1 × TE buffer, pH 8) for 40 min at RT, followed by rinsing with DI water to remove the nonhybridized target cDNA molecules.

The sequences of 20-mer probe ssDNA (5′-GTT-CTT-CTC-ATT-CTT-CCC-CT-3′), complementary target cDNA (5′-AG-GGG-AAG-AAT-GAG-AAG-AAC-3′) and fully mismatched ncDNA (5′-TC-CCC-TTC-TTA-CTC-TTC-TTG-3′) used in this study were purchased from Eurofins (Eurofins MWG Operon, Germany).

3. RESULTS AND DISCUSSION

3.1. Leakage-Current Measurements and Surface-Charge Sensitivity of EIS Chips. The quality of the oxide layer, drift of the output signal and the surface-charge sensitivity of the fabricated SiO_2-gate EIS chips are crucial factors, which should be checked before starting DNA-detection experiments. The quality of the gate-oxide layer has been tested by measuring the leakage current between the reference electrode and rear-side contact of the EIS chip by varying the applied gate voltage in the range from −2 to +2 V. For a correct functioning of the EIS sensors, the leakage current should be very small. Therefore, only chips having leakage current less than 10 nA were chosen for further DNA-detection experiments.

In separate experiments, the drift behavior of the bare SiO_2-gate EIS sensor has been studied. For this, the ConCap signal of the EIS sensor was recorded directly after applying the PBS buffer (pH 7) onto the bare sensor surface and after incubation in the same solution over 7 days. The drift of the EIS sensor was evaluated from the shift of the ConCap curve and amounted to be approximately 8 mV/day. In further experiments on DNA detection, before the surface modification processes, the sensors were conditioned in PBS buffer (or in measurement solution) for at least 12 h, in order to reduce the drift of SiO_2-gate EIS sensors.

Because the surface charge of the SiO_2 is known to be pH-dependent,[50] the charge sensitivity of the EIS chips has been tested via the measurement of shifts of $C-V$ curves along the voltage axis in various pH buffer solutions from pH 5 to pH 9. The pH sensitivity evaluated from these shifts of $C-V$ curves in the depletion region was 42 mV/pH, which is comparable to values previously reported for thermally grown SiO_2 layers (e.g., refs 30, 51). These results demonstrate the suitability of the

DOI: 10.1021/acsami.5b05146
ACS Appl. Mater. Interfaces 2015, 7, 20068−20075

developed EIS devices as charge-sensitive transducers for further experiments on the label-free detection of DNA immobilization and hybridization by their intrinsic molecular charge.

3.2. Surface Characterization of PAH Layer. Figure 3 shows an example of AFM image of the EIS sensor surface after the PAH adsorption. The PAH layer was homogeneous as evidenced by the AFM images taken from different areas of the EIS surface. The cleaned and PAH-covered SiO_2 surfaces were smooth with average rms values of 0.12 and 0.55 nm, respectively. The PAH molecules form a densely packed layer assumedly with a flat conformation of the PAH molecules. However, some pin holes and worm-like structures can be observed on the AFM image of the PAH surface in Figure 3, which is a general phenomenon for LbL-prepared polyelectrolyte films. The average height of the polyelectrolyte layer was ~2−3 nm, which is in agreement with results reported for a PAH layer prepared from 50 μM PAH solution adjusted with 100 mM NaCl.[46]

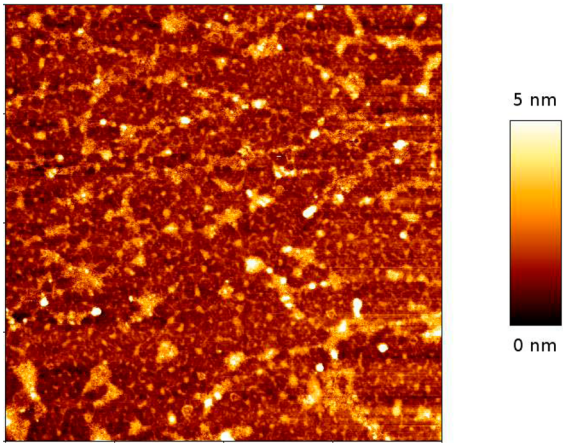

Figure 3. AFM image of the SiO_2 surface covered with PAH layer. Scan size is 2 × 2 μm.

In addition to AFM investigations, the wettability of the sensor surface before and after the cleaning step with piranha solution and after deposition of the PAH layer has been studied by water contact-angle measurements (see Supporting Information). After treatment in piranha solution, the SiO_2 surface becomes highly hydrophilic, which results in a decrease of the contact angle from 89° to less than 10°. The contact angle increases to 34° after the PAH adsorption that is in good agreement with the results reported for the PAH adsorption on a hydrophilic glass substrate.[52]

3.3. Label-Free Detection of PAH Adsorption, Probe ssDNA Immobilization and Target cDNA Hybridization. The capacitive EIS sensors were characterized before and after each surface-modification step by means of $C-V$ and ConCap method. Figure 4 shows an example of label-free electrostatic detection of PAH adsorption, probe ssDNA immobilization and target cDNA hybridization with the EIS sensor. In this experiment, the $C-V$ curves (a) and the ConCap response (b) of the EIS sensor were recorded in 10 mM NaCl solution (pH 5.45) before and after PAH adsorption, after ssDNA immobilization and after subsequent hybridization with target cDNA molecules. The recorded $C-V$ curves exhibit a typical high-frequency shape. Dependent on the magnitude and polarity of the applied gate voltage, V_G, three regions in the $C-V$ curves of the bare and modified EIS sensor can be distinguished: accumulation (V_G<−1.25 V), depletion (−1 V<V_G < 0.1 V) and inversion (V_G > 0.25 V).

The total capacitance of the EIS structure (C_{EIS}) can be represented as a series connection of the geometrical capacitance of the gate insulator (C_i) and the variable space−charge capacitance of the semiconductor (C_{sc}) that depends, among others, on the voltage applied to the gate and the charge (potential) at the gate-insulator/electrolyte interface (the electrochemical double-layer capacitance and capacitance of the adsorbed monolayer are usually much greater than C_i and C_{sc} and can thus, be neglected (e.g., ref 46)). As it can be seen, after surface-modification steps, the maximum capacitance in the accumulation range of the $C-V$ curve remains nearly unchanged ($C_{EIS} \approx C_i$), which is consistent with our previous results on the detection of charged macromolecules or nanoparticles with the capacitive EIS sensor.[24,46] On the other hand, large shifts of $C-V$ curves along the voltage axis have been observed in the depletion range, whereat the direction and magnitude of the shifts depends on the sign and amount of the adsorbed charge. This indicates that the adsorption and binding of charged macromolecules induces an interfacial potential change, resulting in a modulation of the flatband voltage and capacitance of the EIS structure. The binding of positively charged PAH molecules to the negatively charged SiO_2 surface will increase the width of the depletion layer and decrease the space-charge capacitance in the Si, C_{sc}. This will result in a decrease of the total capacitance of the

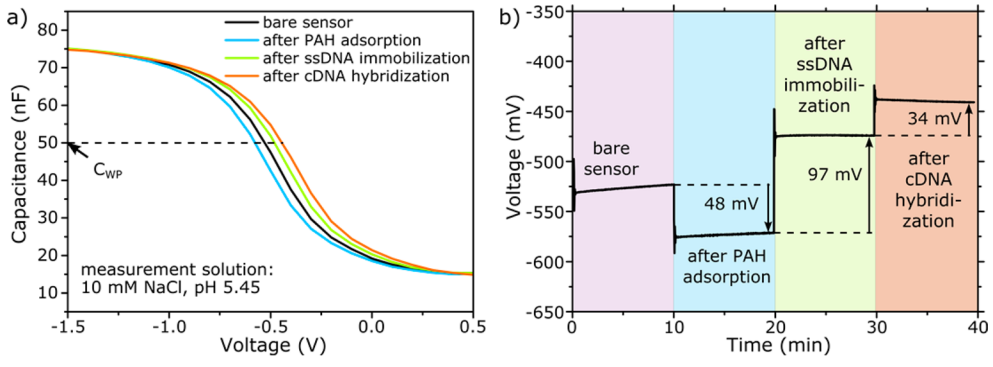

Figure 4. $C-V$ curves (a) and ConCap response (b) of the capacitive p-Si-SiO_2 EIS sensor measured in 10 mM NaCl (pH 5.45) before and after PAH adsorption, after probe ssDNA immobilization and after hybridization with complementary cDNA molecules. Working point (constant capacitance) in depletion region was set to 50 nF.

DOI: 10.1021/acsami.5b05146
ACS Appl. Mater. Interfaces 2015, 7, 20068−20075

sensor and in a shift of the $C-V$ curve in the direction of more negative gate voltages. In contrast, the electrostatic binding of negatively charged probe ssDNA molecules to the positively charged PAH and subsequent hybridization with complementary target cDNAs will lead to a decrease of the width of the depletion layer and an increase of the C_{sc}. As a result, the $C-V$ curve will shift in the direction of more positive (or less negative) gate voltages.

Both the direction and the magnitude of potential shifts can directly be determined from the dynamic ConCap-mode measurements (Figure 4b). In addition, the real-time ConCap response makes the drift behavior of the bare and modified EIS sensor visible. As can be seen, immediately after exposing to the measurement solution, large signal changes induced due to the SiO_2 surface modification by the charged macromolecules have been registered. Then, small signal drift over time has been observed. In most cases, it takes several minutes to achieve equilibrium conditions and a relatively stable signal. Typically, the signal changes induced by the PAH adsorption, DNA-immobilization or hybridization processes were much higher than that of caused due to the drift effect. A ConCap signal of approximately 48 mV was recorded after the adsorption of PAH molecules. The probe ssDNA-immobilization signal was 97 mV. After the hybridization process, the negative charge of the dsDNA molecules is increased, resulting in an additional potential shift (hybridization signal) of 34 mV in the direction of less negative voltages.

Let us estimate the density of probe ssDNA molecules (N_p) adsorbed on the PAH layer using the experimentally measured ssDNA immobilization signal (ΔV_G). Adopting a simplified double-layer capacitor model described in ref. [53] and by assuming that (1) the double-layer capacitance, C_d, remains nearly unchanged after the adsorption of ssDNA molecules, (2) the probe ssDNA molecules are preferentially flat-oriented on the EIS surface with negatively charged phosphate groups directed to the positively charged PAH molecules, and (3) the charges inside the semiconductor and insulator as well as the screening of the DNA charge by counterions in the solution can be neglected, the following simplified relation between the surface potential change ($\Delta\varphi$) and the excess surface charge (ΔQ) can be obtained:[23,24]

$$\Delta V_G \approx \Delta\varphi = \Delta Q/C_d = enN_p/C_d \quad (1)$$

where e is the elementary charge ($e = 1.6 \times 10^{-19}$ C), and n is the number of charged phosphate groups. The density of the adsorbed probe ssDNA molecules calculated from expression (1) amounts to be approximately $N_p = 6 \times 10^{11}$ ssDNA/cm^2, which is in good agreement with results ($N_p = 4 \times 10^{11}$ ssDNA/cm^2) reported for 20-mer DNA molecules covalently attached to the silanized SiO_2 gate surface of an ion-sensitive field-effect transistor.[54] The simulation parameters are ΔV_G = 97 mV (evaluated from the ConCap curve in Figure 4b), n = 20; the double-layer capacitance C_d was taken to be 20 μF/cm^2.[55] The density of hybridized dsDNA molecules calculated using eq 1 and the measured hybridization signal of 34 mV (see Figure 4b) was 2.1×10^{11} dsDNA/cm^2. Thus, the hybridization efficiency amounts to be approximately 35%.

In general, the observed hybridization signal was smaller than the immobilization signal that is in agreement with results reported previously (e.g., refs 37, 56). This effect could be explained by assuming that (1) not all adsorbed probe ssDNA molecules form a flat-oriented elongated structure with DNA nucleobases exposed to the surrounding solution and are ready to hybridize with target cDNA molecules, (2) the charge of dsDNA molecules is partially screened by small counterions in the solution, (3) some hybridized dsDNA molecules detach from the surface, or some combination thereof.

Usually, immobilized probe ssDNA molecules do not form a closely packed, dense layer. Therefore, negatively charged target cDNA or noncomplementary DNA (ncDNA) molecules can electrostatically adsorb onto those positively charged areas of PAH not covered with probe ssDNA, resulting in a false signal. To prevent or reduce an unspecific adsorption of cDNA or ncDNA, the surface areas of PAH not covered with the probe ssDNA have to be blocked by a chemical agent (e.g., bovine serum albumin (BSA)), which inhibits unspecific adsorption. Therefore, after probe ssDNA immobilization, 1% BSA (diluted in DI water, adjusted to pH 5.45) was applied to the chip surface for 60 min at RT, followed by rinsing with measurement solution. At pH 5.45, the BSA molecules are weakly negatively charged, because the isoelectric point of BSA is around pH 4.7.[57] To find out the impact of unspecific adsorption of ncDNA molecules on the EIS signal, after blocking procedure, the sensor surface was exposed to fully mismatched ncDNA solution (5 μM 20-mer ncDNA dissolved in 1 × TE buffer, pH 8) for 40 min at RT, followed by rinsing with DI water.

Figure 5 depicts the ConCap response of an EIS sensor recorded in 1 mM NaCl solution (pH 5.45) before and after PAH adsorption, after probe ssDNA immobilization, after blocking with BSA, after incubation in a solution containing fully mismatched ncDNA molecules (5 μM) and after hybridization of probe ssDNA with target cDNA molecules (5 μM).

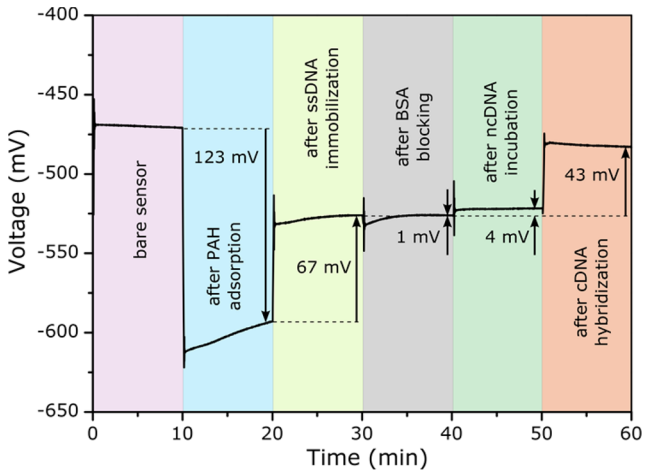

Figure 5. ConCap response of EIS sensor recorded in 1 mM NaCl solution (pH 5.45) before and after PAH adsorption, after probe ssDNA immobilization, after blocking with BSA, after incubation in a solution containing fully mismatched ncDNA molecules (5 μM) and after hybridization of probe ssDNA with target cDNA molecules (5 μM).

The DNA immobilization and hybridization signals evaluated from the ConCap response in Figure 5 were 67 and 43 mV, respectively. At the same time, unspecific adsorption of fully mismatched ncDNA molecules induces only a small potential shift of 4 mV. Thus, the DNA-hybridization signal was more than 10 times higher than the signal generated due to the unspecific adsorption of ncDNA molecules. This experiment demonstrates the specificity of the developed EIS sensor

DOI: 10.1021/acsami.5b05146
ACS Appl. Mater. Interfaces 2015, 7, 20068−20075

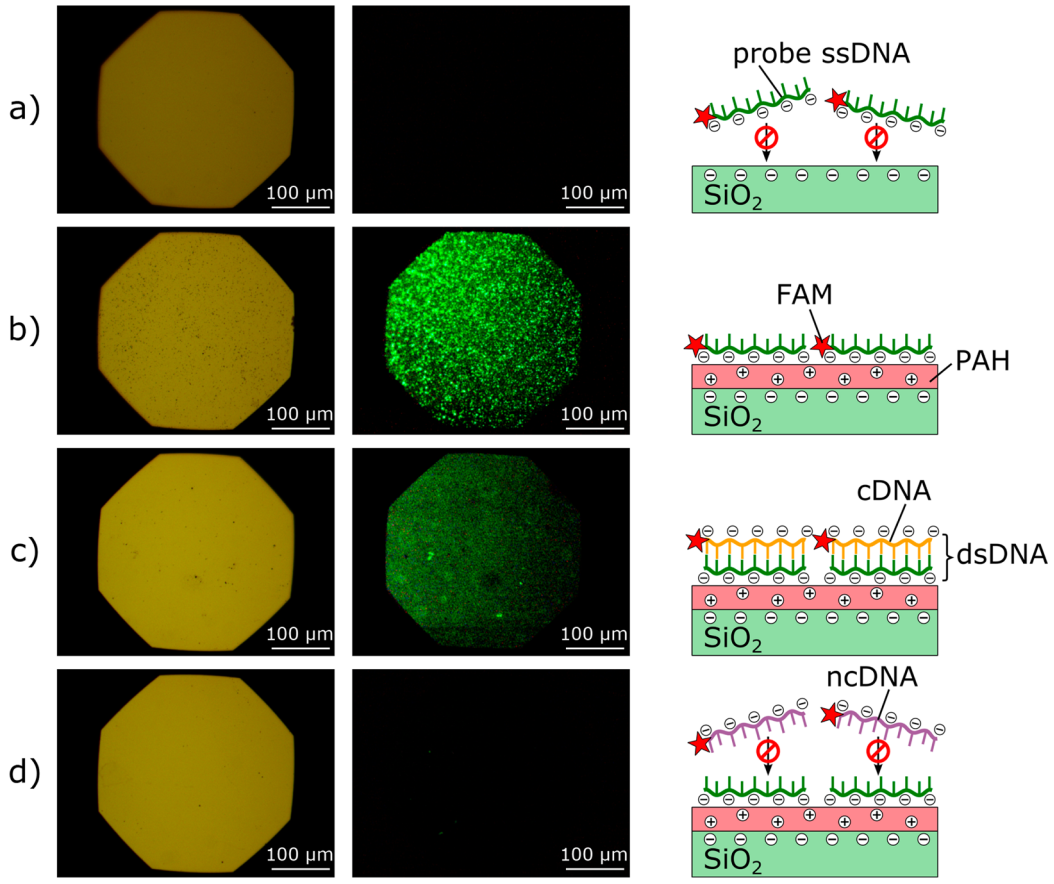

Figure 6. (Left column) Light-field and (middle column) fluorescence-mode images after exposing the (a) bare and (b) PAH-modified EIS sensor to FAM-labeled probe ssDNA solution as well as after incubation of the EIS sensor modified with PAH/probe-ssDNA bilayer with the solution of FAM-labeled (c) cDNA or (d) ncDNA molecules. The schematics in the right column visualize the corresponding binding tendency. For each fluorescence experiment, a separate EIS chip was used.

capable of distinguishing the complementary cDNA from fully mismatched ncDNA. As expected, due to the less-effective Debye screening effect in a low-ionic strength solution, the hybridization signal measured in a 1 mM solution (Debye length $\lambda_D \approx 10$ nm) was higher (43 mV) than that of recorded in a 10 mM solution ($\lambda_D \approx 3$ nm; 34 mV; Figure 4b).

3.4. Fluorescence Measurements. In addition to field-effect characterization of EIS-based DNA sensors by means of $C-V$ and ConCap methods, fluorescence measurements were performed as a reference method to verify the DNA-immobilization and hybridization event using an Axio Imager A1m (Carl Zeiss AG, Germany) fluorescence microscope with respective filter set. To visualize the successful DNA immobilization onto the PAH layer, probe ssDNA (20-mer) were modified with the fluorescence dye 6-carboxyfluorescein (FAM). For verification of the hybridization reaction, first unmodified 20-mer probe ssDNA molecules were immobilized onto the surface of the PAH-modified EIS sensor, then the sensor was exposed to the solution containing FAM-modified target cDNA or ncDNA (also 20-mer), respectively. All surface-modification and washing steps were performed according to the protocols described above for electrochemical experiments.

Figure 6 shows the results of fluorescence measurements after exposing the bare and PAH-modified EIS-sensor surface to FAM-labeled probe ssDNA solution (5 μM) as well as after incubation of the EIS sensor modified with a PAH/probe-ssDNA bilayer with the 5 μM solution of FAM-labeled cDNA or ncDNA molecules. No fluorescence signal has been detected after exposing the bare EIS sensor to FAM-labeled probe ssDNA solution (Figure 6a). The electrostatic repulsion between the probe ssDNA and SiO_2 surface (both are negatively charged) prevents the immobilization process. As a consequence, no FAM-labeled ssDNA molecules remain on the sensor surface after the washing step. In contrast, a bright and homogeneous fluorescence signal was observed after incubation of the PAH-modified EIS sensor surface to FAM-labeled probe ssDNA solution (Figure 6b), verifying a successful immobilization of probe ssDNA molecules onto the positively charged PAH layer. The fluorescence signal has also been observed even after six washing steps, without any loss of fluorescence intensity. In comparison to Figure 6b, a less bright fluorescence signal has been detected after hybridization of probe ssDNA with FAM-labeled cDNA (Figure 6c). This experiment verifies, on one hand, the successful hybridization process; on the other hand, it indicates that not all immobilized probe ssDNA molecules were hybridized with the target cDNA molecules (i.e., the hybridization efficiency was <100%), supporting the results of electrochemical measurements (see section 3.3). As expected, practically no fluorescence signal has been detected after incubation of the EIS sensor modified with PAH/probe-ssDNA bilayer with the FAM-labeled ncDNA solution (Figure 6d) that is also in good correlation with the electrochemical measurements presented in Figure 5.

DOI: 10.1021/acsami.5b05146
ACS Appl. Mater. Interfaces 2015, 7, 20068−20075

CONCLUSIONS

Among various concepts proposed for the label-free detection of DNA immobilization and hybridization, the semiconductor field-effect device platform, which is based on the electrostatic detection of DNA molecules by their intrinsic negative charge, is one of the most attractive approaches. In this work, a capacitive EIS sensor consisting of an Al−p-Si−SiO_2 structure modified with a weak polyelectrolyte layer of PAH has successfully been applied for label-free electrical detection of DNA immobilization and hybridization. The LbL technique was used for the electrostatic adsorption of positively charged PAH macromolecules on the negatively charged SiO_2 layer as well as for an easy and fast immobilization of negatively charged probe ssDNA molecules onto the positively charged PAH layer. The surface morphology of the PAH layer was studied by AFM and contact-angle measurements; the EIS sensors were electrochemically characterized in the same measurement solution (1 mM or 10 mM NaCl, pH 5.45) after each surface-modification process (PAH adsorption, probe ssDNA immobilization, hybridization with cDNA, BSA blocking, unspecific adsorption of ncDNA) by means of *C*−*V* and ConCap method. Large potential shifts of 97 and 34 mV have been observed after LbL immobilization of probe ssDNA onto the positively charged PAH layer and subsequent hybridization with cDNA, respectively. The density of probe ssDNA and dsDNA molecules, estimated using the experimentally determined DNA-immobilization and hybridization signals together with a simplified double-layer capacitor model, were 6×10^{11} cDNA/cm^2 and 2.1×10^{11} dsDNA/cm^2, respectively. The hybridization efficiency estimated using the measured immobilization and hybridization signals is 35%. The advantage of the adsorptive immobilization technique is that both the probe ssDNA as well as dsDNA (after hybridization) molecules preferentially lie flat near to the EIS surface with molecular charges positioned within the Debye length from the gate surface, resulting in a higher sensor signal. The hybridization signal increases from 34 to 43 mV with decreasing the ionic strength of the solution from 10 to 1 mM NaCl. At the same time, a small potential shift of 4 mV was recorded in the case of unspecific adsorption of fully mismatched ncDNA. This demonstrates the ability of capacitive EIS sensors to distinguish between complementary and mismatched DNA sequences. The results of field-effect experiments were supported by fluorescence measurements serving as a reference method to verify the DNA-immobilization and hybridization event.

The obtained results underline the potential of the capacitive EIS as a promising transducer platform for label-free electrical detection of DNA molecules by their intrinsic molecular charge. Future work will be directed to study the lower detection limit as well as to realize an array of capacitive EIS sensors in a differential-mode setup for the accurate detection of single-nucleotide polymorphisms.

ASSOCIATED CONTENT

Supporting Information

The Supporting Information is available free of charge on the ACS Publications website at DOI: 10.1021/acsami.5b05146.

Contact-angle measurements details. (PDF)

AUTHOR INFORMATION

Corresponding Author

* E-mail: a.poghossian@fz-juelich.de.

Notes

The authors declare no competing financial interest.

ACKNOWLEDGMENTS

This work was funded by the Bundesministerium für Bildung und Forschung (DiaCharge project 031A192D). C.W. thanks the National Natural Science Foundation of China (Grant 31470956), and the Zhejiang Provincial Natural Science Foundation of China (Grant LY13H180002) for financial support. The authors gratefully thank the Institute of Applied Polymer Chemistry (FH Aachen) for technical support by contact-angle experiments, H. Iken for fabrication of EIS sensors and M. Bäcker for AFM measurements.

REFERENCES

(1) Sassolas, A.; Leca-Bouvier, B. D.; Blum, L. J. DNA Biosensors and Microarrays. *Chem. Rev.* **2008**, *108*, 109−139.
(2) Wei, F.; Lillehoj, P. B.; Ho, C. M. DNA Diagnostics: Nanotechnology-enhanced Electrochemical Detection of Nucleic Acids. *Pediatr. Res.* **2010**, *67*, 458−468.
(3) Choi, S.; Goryll, M.; Sin, L. Y. M.; Wong, P. K.; Chae, J. Microfluidic-based Biosensors toward Point-of-care Detection of Nucleic Acids and Proteins. *Microfluid. Nanofluid.* **2011**, *10*, 231−247.
(4) Poghossian, A.; Schöning, M. J. Label-free Sensing of Biomolecules with Field-effect Devices for Clinical Applications. *Electroanalysis* **2014**, *26*, 1197−1213.
(5) Song, L.; Ahn, S.; Walt, D. R. Fiber-optic Microsphere-based Arrays for Multiplexed Biological Warfare Agent Detection. *Anal. Chem.* **2006**, *78*, 1023−1033.
(6) Mao, X. L.; Yang, L. J.; Su, X. L.; Li, Y. B. A Nanoparticle Amplification Based Quartz Crystal Microbalance DNA Sensor for Detection of Escherichia Coli O157: H7. *Biosens. Bioelectron.* **2006**, *21*, 1178−1185.
(7) Cagnin, S.; Caraballo, M.; Guiducci, C.; Martini, P.; Ross, M.; Santaana, M.; Danley, D.; West, T.; Lanfranchi, G. Overview of Electrochemical DNA Biosensors: New Approaches to Detect the Expression of Life. *Sensors* **2009**, *9*, 3122−3148.
(8) Nelson, B. P.; Grimsrud, T. E.; Liles, M. R.; Goodman, R. M.; Corn, R. M. Surface Plasmon Resonance Imaging Measurements of DNA and RNA Hybridization Adsorption onto DNA Microarrays. *Anal. Chem.* **2001**, *73*, 1−7.
(9) Lazerges, M.; Bedioui, F. Analysis of the Evolution of the Detection Limits of Electrochemical DNA Biosensors. *Anal. Bioanal. Chem.* **2013**, *405*, 3705−3714.
(10) Park, J. Y.; Park, S. M. DNA Hybridization Sensors Based on Electrochemical Impedance Spectroscopy as a Detection Tool. *Sensors* **2009**, *9*, 9513−9532.
(11) Riedel, M.; Kartchemnik, J.; Schöning, M. J.; Lisdat, F. Impedimetric DNA Detection—Steps forward to Sensorial Application. *Anal. Chem.* **2014**, *86*, 7867−7874.
(12) Mehrabani, S.; Maker, A. J.; Armani, A. M. Hybrid Integrated Label-free Chemical and Biological Sensors. *Sensors* **2014**, *14*, 5890−5928.
(13) Wu, C. C.; Ko, F. H.; Yang, Y. S.; Hsia, D. L.; Lee, B. S.; Su, T. S. Label-free Biosensing of a Gene Mutation Using a Silicon Nanowire Field-effect Transistor. *Biosens. Bioelectron.* **2009**, *25*, 820−825.
(14) Poghossian, A. The Super-Nernstian pH Sensitivity of Ta_2O_5-Gate ISFETs. *Sens. Actuators, B* **1992**, *7*, 367−370.
(15) Poghossian, A.; Baade, A.; Emons, H.; Schoning, M. J. Application of ISFETs for pH Measurement in Rain Droplets. *Sens. Actuators, B* **2001**, *76*, 634−638.
(16) Poghossian, A.; Mai, D. T.; Mourzina, Y.; Schöning, M. J. Impedance Effect of an Ion-sensitive Membrane: Characterisation of an EMIS Sensor by Impedance Spectroscopy, Capacitance-voltage and Constant-capacitance Method. *Sens. Actuators, B* **2004**, *103*, 423−428.
(17) Jimenez-Jorquera, C.; Orozco, J.; Baldi, A. ISFET Based Microsensors for Environmental Monitoring. *Sensors* **2010**, *10*, 61−83.

DOI: 10.1021/acsami.5b05146
ACS Appl. Mater. Interfaces 2015, 7, 20068−20075

(18) Gun, J.; Schöning, M. J.; Abouzar, M. H.; Poghossian, A.; Katz, E. Field-effect Nanoparticle-based Glucose Sensor on a Chip: Amplification Effect of Coimmobilized Redox Species. *Electroanalysis* **2008**, *20*, 1748−1753.
(19) Lee, C. S.; Kim, S. K.; Kim, M. Ion-sensitive Field-effect Transistor for Biological Sensing. *Sensors* **2009**, *9*, 7111−7131.
(20) Siqueira, J. R.; Abouzar, M. H.; Bäcker, M.; Zucolotto, V.; Poghossian, A.; Oliveira, O. N.; Schöning, M. J. Carbon Nanotubes in Nanostructured Films: Potential Application as Amperometric and Potentiometric Field-effect (Bio-)Chemical Sensors. *Phys. Status Solidi A* **2009**, *206*, 462−467.
(21) Nakazato, K. An Integrated ISFET Sensor Array. *Sensors* **2009**, *9*, 8831−8851.
(22) Stern, E.; Vacic, A.; Reed, M. A. Semiconducting Nanowire Field-effect Transistor Biomolecular Sensors. *IEEE Trans. Electron Devices* **2008**, *55*, 3119−3130.
(23) Gun, J.; Gutkin, V.; Lev, O.; Boyen, H. G.; Saitner, M.; Wagner, P.; D'Olieslaeger, M.; Abouzar, M. H.; Poghossian, A.; Schöning, M. J. Tracing Gold Nanoparticle Charge by Electrolyte-Insulator-Semiconductor Devices. *J. Phys. Chem. C* **2011**, *115*, 4439−4445.
(24) Poghossian, A.; Bäcker, M.; Mayer, D.; Schöning, M. J. Gating Capacitive Field-effect Sensors by the Charge of Nanoparticle/Molecule Hybrids. *Nanoscale* **2015**, *7*, 1023−1031.
(25) Fritz, J.; Cooper, E. B.; Gaudet, S.; Sorger, P. K.; Manalis, S. R. Electronic Detection of DNA by its Intrinsic Molecular Charge. *Proc. Natl. Acad. Sci. U. S. A.* **2002**, *99*, 14142−14146.
(26) Ingebrandt, S.; Han, Y.; Nakamura, F.; Poghossian, A.; Schöning, M. J.; Offenhäusser, A. Label-free Detection of Single Nucleotide Polymorphisms Utilizing the Differential Transfer Function of Field-effect Transistors. *Biosens. Bioelectron.* **2007**, *22*, 2834−2840.
(27) Hahm, J.; Lieber, C. M. Direct Ultrasensitive Electrical Detection of DNA and DNA Sequence Variations Using Nanowire Nanosensors. *Nano Lett.* **2004**, *4*, 51−54.
(28) Kataoka-Hamai, C.; Miyahara, Y. Label-free Detection of DNA by Field-effect Devices. *IEEE Sens. J.* **2011**, *11*, 3153−3160.
(29) Lu, N.; Gao, A.; Dai, P.; Li, T.; Wang, Y.; Gao, X.; Song, S.; Fan, C.; Wang, Y. Ultra-sensitive Nucleic Acids Detection with Electrical Nanosensors Based on CMOS-compatible Silicon Nanowire Field-effect Transistors. *Methods* **2013**, *63*, 212−218.
(30) Abouzar, M. H.; Poghossian, A.; Cherstvy, A. G.; Pedraza, A. M.; Ingebrandt, S.; Schöning, M. J. Label-free Electrical Detection of DNA by Means of Field-effect Nanoplate Capacitors: Experiments and Modeling. *Phys. Status Solidi A* **2012**, *209*, 925−934.
(31) Kulkarni, A.; Xu, Y.; Ahn, C.; Amin, R.; Park, S. H.; Kim, T.; Lee, M. The Label-free DNA Sensor Using a Silicon Nanowire Array. *J. Biotechnol.* **2012**, *160*, 91−96.
(32) Wu, C. S.; Bronder, T.; Poghossian, A.; Werner, C. F.; Schöning, M. J. Label-free Detection of DNA Using a Light-addressable Potentiometric Sensor Modified with a Positively Charged Polyelectrolyte Layer. *Nanoscale* **2015**, *7*, 6143−6150.
(33) Barbaro, M.; Caboni, A.; Loi, D.; Lai, S.; Homsy, A.; van der Wal, P. D.; de Rooij, N. F. Label-free, Direct DNA Detection by Means of a Standard CMOS Electronic Chip. *Sens. Actuators, B* **2012**, *171−172*, 148−154.
(34) Adam, T.; Hashim, U. Highly Sensitive Silicon Nanowire Biosensor with Novel Liquid Gate Control for Detection of Specific Single-stranded DNA Molecules. *Biosens. Bioelectron.* **2015**, *67*, 656−661.
(35) Veigas, B.; Fortunato, E.; Baptista, P. V. Field Effect Sensors for Nucleic Acid Detection: Recent Advances and Future Perspectives. *Sensors* **2015**, *15*, 10380−10398.
(36) Kuga, S.; Yang, J. H.; Takahashi, H.; Hirama, K.; Iwasaki, T.; Kawarada, H. Detection of Mismatched DNA on Partially Negatively Charged Diamond Surfaces by Optical and Potentiometric Methods. *J. Am. Chem. Soc.* **2008**, *130*, 13251−13263.
(37) Liu Y.; Dutton, R. W. Effects of Charge Screening and Surface Properties on Signal Transduction in Field Effect Nanowire Biosensors. *J. Appl. Phys.* **2009**, *106*, 01470110.1063/1.3156657
(38) Zhang, G. J.; Zhang, G.; Chua, J. H.; Chee, R. E.; Wong, E. H.; Agarwal, A.; Buddharaju, K. D.; Singh, N.; Gao, Z.; Balasubramanian, N. DNA Sensing by Silicon Nanowire: Charge Layer Distance Dependence. *Nano Lett.* **2008**, *8*, 1066−1070.
(39) Rant, U.; Arinaga, K.; Fujita, S.; Yokoyama, N.; Abstreiter, G.; Tornow, M. Electrical Manipulation of Oligonucleotides Grafted to Charged Surfaces. *Org. Biomol. Chem.* **2006**, *4*, 3448−3455.
(40) Uno, S.; Iio, M.; Ozawa H.; Nakazato, K. Full Three-dimensional Simulation of Ion-sensitive Field-effect Transistor Flatband Voltage Shifts Due to DNA Immobilization and Hybridization. *Jpn. J. Appl. Phys.* **2010**, *49*, 01AG0710.1143/JJAP.49.01AG07
(41) Nishio, Y.; Uno, S.; Nakazato, K. Three-dimensional Simulation of DNA Sensing by Ion-sensitive Field-effect Transistor: Optimization of DNA Position and Orientation. *Jpn. J. Appl. Phys.* **2013**, *52*, 04CL0110.7567/JJAP.52.04CL01
(42) Evtugyn, G. A.; Hianik, T. Layer-by-layer Polyelectrolyte Assembles Involving DNA as a Platform for DNA Sensors. *Curr. Anal. Chem.* **2011**, *7*, 8−34.
(43) Bunimovich, Y. L.; Shin, Y. S.; Yeo, W.; Amori, M.; Kwong, G.; Heath, J. R. Quantitative Real-time Measurements of DNA Hybridization with Alkylated Nonoxidized Silicon Nanowires in Electrolyte Solution. *J. Am. Chem. Soc.* **2006**, *128*, 16323−16331.
(44) Braeken, D.; Reekmans, G.; Zhou, C.; van Meerbergen, B.; Callewaert, G.; Borghs, G.; Bartic, C. Electronic DNA Hybridisation Detection in Low-ionic Strength Solutions. *J. Exp. Nanosci.* **2008**, *3*, 157−169.
(45) Wang, J.; Zhou, Y. L.; Watkinson, M.; Gautrot, J.; Krause, S. High-sensitivity Light-addressable Potentiometric Sensors Using Silicon on Sapphire Functionalized with Self-assembled Organic Monolayers. *Sens. Actuators, B* **2015**, *209*, 230−236.
(46) Poghossian, A.; Weil, M.; Cherstvy, A. G.; Schöning, M. J. Electrical Monitoring of Polyelectrolyte Multilayer Formation by Means of Capacitive Field-effect Devices. *Anal. Bioanal. Chem.* **2013**, *405*, 6425−6436.
(47) Schönhoff, M.; Ball, V.; Bausch, A. R.; Dejugnat, C.; Delorme, N.; Glinel, K.; Klitzing, R. V.; Steitz, R. Hydration and Internal Properties of Polyelectrolyte Multilayers. *Colloids Surf., A* **2007**, *303*, 14−29.
(48) Meixner, L. K.; Koch, S. Simulation of ISFET Operation Based on the Site-binding Model. *Sens. Actuators, B* **1992**, *6*, 315−318.
(49) Smith, R. N.; McCormick, M.; Barrett, C. J.; Reven, L.; Spiess, H. W. NMR Studies of PAH/PSS Polyelectrolyte Multilayers Adsorbed onto Silica. *Macromolecules* **2004**, *37*, 4830−4838.
(50) Bergveld, P. Thirty Years of ISFETOLOGY: What Happened in the Past 30 Years and What May Happen in the Next 30 Years. *Sens. Actuators, B* **2003**, *88*, 1−20.
(51) Cane, C.; Gracia, I.; Merlos, A. Microtechnologies for pH ISFET Chemical Sensors. *Microelectron. J.* **1997**, *28*, 389−405.
(52) Yoo, D.; Shiratori, S.; Rubner, M. Controlling Bilayer Composition and Surface Wettability of Sequentially Adsorbed Multilayers of Weak Polyelectrolytes. *Macromolecules* **1998**, *31*, 4309−4318.
(53) van Hal, R. E. G.; Eijkel, J. C. T.; Bergveld, P. A General Model to Describe the Electrostatic Potential at Electrolyte Oxide Interfaces. *Adv. Colloid Interface Sci.* **1996**, *69*, 31−62.
(54) Uslu, F.; Ingebrandt, S.; Mayer, D.; Böcker-Meffert, S.; Odenthal, M.; Offenhäusser, A. Labelfree Fully Electronic Nucleic Acid Detection System Based on a Field-effect Transistor Device. *Biosens. Bioelectron.* **2004**, *19*, 1723−1731.
(55) Einati, H.; Mottel, A.; Inberg, A.; Shacham-Diamand, Y. Electrochemical Studies of Self-assembled Monolayers Using Impedance Spectroscopy. *Electrochim. Acta* **2009**, *54*, 6063−6069.
(56) Ingebrandt, S.; Vu, X. T.; Eschermann, J. F.; Stockmann, R.; Offenhäusser, A. Top-down Processed SOI Nanowire Devices for Biomedical Applications. *ECS Trans.* **2011**, *35*, 3−15.
(57) Ge, S.; Kojio, K.; Takahara, A.; Kajiyama, T. Bovine Serum Albumin Adsorption onto Immobilized Organotrichlorosilane Surface: Influence of the Phase Separation on Protein Adsorption Patterns. *J. Biomater. Sci., Polym. Ed.* **1998**, *9*, 131−150.

DOI: 10.1021/acsami.5b05146
ACS Appl. Mater. Interfaces 2015, 7, 20068−20075